Journal of Applied Data Sciences
Vol. 7, No. 3, September 2026, pp. 2035-2051

Comparative Analysis of YOLOv8s and Faster R-CNN for High-Resolution UAV RGB Oil Palm Health Detection: Accuracy versus Inference Speed Trade-Off

Kristia Yuliawan[1,*], Danny Manongga[2], Hendry[3]

[1,2,3]*Department of Information Technology, Satya Wacana Christian University, Salatiga, Indonesia*

(Received: February 1, 2026; Revised: March 25, 2026; Accepted: June 20, 2026; Available online: July 20, 2026)

Abstract

Accurate and rapid detection of oil palm health conditions using UAV imagery is essential for supporting precision agriculture and large-scale plantation monitoring. However, challenges such as overlapping canopies, complex background textures, varying illumination, and severe class imbalance often reduce the reliability of automated detection systems. This study presents a comparative evaluation between YOLOv8s, a one-stage object detector, and Faster R-CNN, a two-stage detector, for identifying healthy and unhealthy oil palm trees using high-resolution UAV RGB imagery. The dataset consists of 2,303 annotated images collected from drone surveys and divided into training (70%), validation (20%), and testing (10%) subsets under a controlled experimental design. Both models were trained and evaluated using identical preprocessing pipelines and annotation formats to ensure fairness in comparison. Performance was assessed using precision, recall, F1-score, mean Average Precision (mAP@50 and mAP@50–95), and inference time. Experimental results show that YOLOv8s achieves superior performance with 0.987 precision, 0.998 recall, 0.977 mAP@50–95, and extremely fast inference speed of 1.1 ms per image. In contrast, Faster R-CNN achieves comparable detection accuracy at 0.981 precision and 0.993 recall but with significantly higher computational cost, reaching 875 ms per image. These findings indicate that YOLOv8s provides an optimal balance between accuracy and efficiency, making it more suitable for real-time UAV-based monitoring systems, while Faster R-CNN is more appropriate for offline and high-precision analytical tasks. The study contributes a standardized benchmarking framework for deep learning-based oil palm health detection and provides practical insights for selecting appropriate models in smart agricultural applications.

Keywords: UAV Remote Sensing, Precision Agriculture, Object Detection, Oil Palm Health Monitoring, Yolov8s, Faster R-CNN, Deep Learning, Aerial Imagery

1. Introduction

It's important to regularly monitor the health of oil palm plantations through timely and reliable means. This is because if plant stress, pest infestation, or disease symptoms go undetected for a long time, there will be a considerable drop in productivity along with the inefficiency of input and loss of sustainability. UAV (drone) imagery has recently emerged as an essential element of precision agriculture since it can obtain detailed information about the whole plantation easily and consistently as opposed to human inspection [1]. UAV images of oil palm plantations help to spot changes in leaf color, unusual crown shapes, and other stress-related signs of the plants. These signs could hardly be revealed through ground-level observation [2]. Thus, supplementing UAV images by automated image analysis is becoming more and more essential in the data-driven plantation management.

This study aims at the automatic detection of health and disease of oil palms segments from drone images at very high-resolution in RGB. Indeed, UAV remote sensing offers a good level of details in the images, yet the health detection of oil palms is still a challenging task due mainly to overlapping crowns, irregular shadows, and changes in illumination in plantation scenes, as well as different viewing angles, and a severe imbalance between healthy and unhealthy samples. These factors might negatively affect detection reliability in scenarios when the model generates false positives, overlooks small unhealthy objects or cannot accurately locate plant crowns. Therefore, a good detection

*Corresponding author: Kristia Yuliawan (982021003@student.uksw.edu)
DOI: https://doi.org/10.47738/jads.v7i3.1430

model should be capable of very precise identification, thorough recall, accurate bounding-box localization, and rapid inference so that it can be used for practical smart agriculture monitoring.

The recent studies indicate that deep learning has taken the lead among methods for automatic object detection in agricultural imagery mainly because of its capability to learn spatial, color, and texture features directly from the image data [3]. For UAV-based monitoring of crops, though the use of one-stage detectors like the YOLO family has been predominant due to their quick results and compatibility for deployment in near real-time, the two-stage detectors like Faster R-CNN still have their place as their region proposal mechanism facilitates thorough object verification [4], [5]. Prior works in agriculture have also shown that using deep learning models can outperform traditional visual inspection or techniques based on handcrafted feature extraction for operations like crop disease and pest detection, tree canopy mapping, and field-level decision support [6]. The study results provide evidence that YOLOv8 and Faster R-CNN can be considered as very good options for UAV-based palm oil health detection.

Still, the literature fails to provide a clear and standardized comparison of YOLOv8s and Faster R-CNN in detecting the health conditions of oil palms using the same UAV image dataset, annotation protocol, and evaluation setting, despite these advances. Most of the aspects of such studies are limited to a single model or they compare newer detectors with older CNN-based or YOLO variants, or they simply report accuracy without a balanced discussion of localization quality and computational speed. This gap matters a lot because a model with high detection accuracy may not be suitable for field operation if the inference is too slow, on the contrary, a faster one may be unreliable if it misses unhealthy palms or makes weak localization even under strict IoU thresholds. Hence, a field-oriented comparison is necessary to shed light on the accuracy-speed trade-off for the effective monitoring of oil palms.

Consequently, this study is focused on the numerical comparison of YOLOv8s and Faster R-CNN being used for detection of healthy and unhealthy oil palm trees via high-resolution UAV RGB images. The study employs 2, 303 annotated images which are split into the training, validation and testing subsets while the same preprocessing and labeling protocol are employed for all. Then, the two models are evaluated by precision, recall, mAP@50, mAP@50-95, loss convergence, and inference time. The primary contribution of this paper is a unified performance evaluation that clearly points out which model delivers the best compromise between detection accuracy and computational efficiency for smart agriculture applications. The findings will hopefully assist in the decision making of deep learning model selection for real-time UAV-based oil palm health monitoring as well as for offline verification scenarios that require a more detailed object analysis.

2. Literature Review

Aerial imagery captured through the use of drones at high resolution can help in the identification of subtle visual changes in the canopy, such as leaf discoloration, necrosis patterns, or reduced vegetation vitality, which are not yet visible to the naked eye, over large plantation areas.[7], [8]. Not only does this method decrease dependence on the experts in the field who are expensive and take too much time, it also raises the precision of the early identification of the plant diseases that jeopardize the production of palm oil. As a result, it allows calling intervention on time and promotes the use of data in smart agriculture [9].

2.1. Drones for smart agriculture

Integrating plant stress remote sensing with AI can enable detecting stressed plants at their very early stages, even prior to showing visible symptoms, drones or Unmanned Aerial Vehicles (UAVs), in fact, are indispensable in this sort of work as they allow to take very quickly high-resolution aerial photos of very large plantation areas, particularly oil palm farms, which are extremely difficult for human inspection [10]. Also, if the UAVs are able to detect real-time plant health changes, there will be less need for manual labor and the subjectivity of field diagnosis can be done away with, and that, in turn, may result in more sustainable agricultural practices and improved operational efficiency of modern plantations [11]. Moreover, drones contribute a lot in smart agriculture applications by making data-based decision-making more effective, as a result of providing more detailed and measurable visual information [12].

One of the biggest issues that come up with the use of UAVs is the need for automatic analysis of the enormous number of photos that are taken in each monitoring session which is simply not humanly possible and also beyond the capabilities of even conventional machine learning models [13]. Deep learning is the method of choice since, besides giving the model the capability to learn the features automatically, it also assists in identifying the very complex patterns of palm oil diseases which are usually visually quite similar [14]. YOLOv8 and Faster R-CNN are two types of models that, from the point of view of detection speed and classification accuracy, have different computational advantages and, for this reason, they are very much suitable for a comparison to determine the best approach for UAV-based crop health assessment [15]. This research aims at increasing the accuracy, speed, and potential for further development of agricultural monitoring systems in a smart farm environment by assessing the performance of the two models using images of oil palm plantations [16].

2.2. Deep Learning Model in the field of Oil Palm Plantation

Background Studies point out that combining deep learning models with aerial photography from drones is currently the main way to check oil palm crop health [29]. In fact, analysis of high-resolution UAV data first involved extracting visual features from the oil palm canopy to warn the problems caused by biotic and abiotic factors, such as pest infestations like bagworms and Oryctes rhinoceros, Ganoderma disease, nutritional deficiencies, and water stress [17]. Different deep learning architectures like CNN, Faster R-CNN, RetinaNet, YOLOv3, and YOLOv8 have shown that they can pattern complex features spatially that humans through traditional analysis or with low-resolution satellite data cannot detect [18]. These works demonstrate that deep learning gives better detection accuracy, works well in different field conditions (generalization), and can handle large plantations with big processing requirements (efficiency), thus making them a vital basis for the introduction of smart farming in the current palm oil industry. Table 1 shows the relevant models and accuracies measured with different metrics. Some papers listed in the table used multiple models; however, the table only shows the model with the highest accuracy.

Table 1. The most relevant deep learning models and their performances.

Ref	Context	Method	Evaluation Metric	Value	Dataset	Year	Selection Rationale
[19]	Oil-palm tree detection (UAV, single/multi-species)	Enhanced RetinaNet	F1-score	94.7%	UAV RGB images	2022	Demonstrated high F1 for multi-species palm detection
[6]	Palm tree detection using Mask R-CNN (Indonesia)	Mask R-CNN	Accuracy	90.52%	UAV imagery	2024	Included due to precision evaluation on real-world plantation
[20]	Health classification of oil-palm trees (healthy/unhealthy)	Faster R-CNN	Precision/Recall/F1	≈0.9+ per class	UAV RGB	2023	Relevant for binary health classification
[21]	Multi-class palm condition classification (MOPAD, UAV)	YOLOv8 (multi-class)	mAP@0.5 / F1-score	Train≈0.99; Web-app: F1≈0.76	MOPAD UAV	2021	Selected for comparative multi-class evaluation
[18]	BSR disease detection using ensemble CNN	DenseNet161 (best ensemble)	Validation Accuracy	91.75%	UAV hyperspectral	2024	Provides ensemble approach reference
[22]	Healthy vs unhealthy palm detection (Faster R-CNN)	Faster R-CNN	Precision/Recall/F1/mAP@0.5	F1=0.79; mAP=0.78	UAV RGB	2025	Relevant for single-class binary health detection
[23]	Early BSR infection detection using hyperspectral UAV	Random Forest	Precision/Recall/F1	F1>0.8 per class	UAV hyperspectral	2022	Early detection study included for performance comparison
[24]	Real-time palm detection on edge device (YOLOv8n)	YOLOv8n	Precision / Recall / mAP@0.5	Prec 95.6%; Rec 93.3%; mAP 98%	Edge-deployed UAV images	2025	Included for real-time deployment relevance

[25]	YOLOv8 vs YOLOv9 for health classification	YOLOv8 & YOLOv9	mAP@0.5, Precision, Recall	YOLOv8: mAP 0.993; YOLOv9: 0.987	UAV RGB	2025	Comparative study between state-of-the-art YOLO versions

3. Methodology

The research flow of this study, depicted in figure 1, starts with capturing plant images using a UAV, then, the images are going through the pre-processing rectification, segmentation, and enhancement of the images to make the data ready for use [26]. Further, model training was done with two main algorithms, Yolov8 and Faster R-CNN, which were again used in the plant health detection phase [27]. The detection results are checked with performance metrics such as accuracy, precision, memory, and F1 score, then they are compared in terms of detection accuracy, processing speed, and computational efficiency [28]. The last step is a final result analysis that focused on the finding of the best model and a trade-off evaluation between accuracy and efficiency to make sure the selection of the best model to support UAV-based crop health monitoring and machine learning [29], [30].

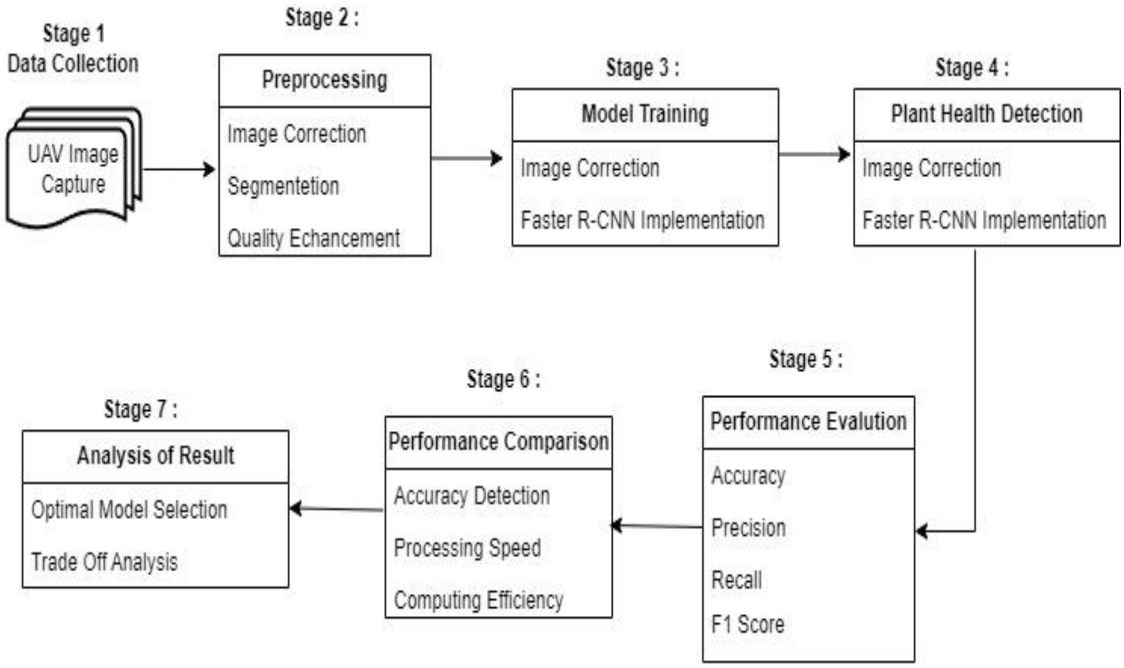

Figure 1. Research Flow

3.1. Algorithmic Pseudocode of the Research Process

To make the workflow in figure 1 operationally reproducible, Algorithm 1 formalizes the complete experimental procedure from UAV image acquisition, data preprocessing, class-imbalance handling, model training, and controlled benchmarking to final accuracy-speed trade-off analysis.

Algorithm 1. Pseudocode of the proposed UAV-based oil palm health detection research process

Input: UAV RGB images D, ground-truth annotations A, flight-block IDs B, class labels C = {Healthy, Unhealthy}
Output: trained model checkpoints, performance metrics, and selected model M*

```
1: BEGIN
2: Acquire high-resolution UAV RGB images of oil palm plantation areas.
3: Assign each image to its corresponding flight block to preserve spatial independence.
4: Split D by non-overlapping flight blocks into training, validation, and testing subsets using a 70:20:10 ratio.
5: FOR each image I_i in D DO
```

Resize I_i to the target input resolution and normalize its visual quality.
Apply denoising and contrast adjustment to reduce illumination and UAV-capture artifacts.
Annotate each oil palm object using bounding boxes and assign the label Healthy or Unhealthy.
Export annotations into YOLO format for YOLOv8s and COCO JSON format for Faster R-CNN.
END FOR
Compute class distribution and identify the Healthy-to-Unhealthy imbalance ratio.
Apply image-level weighted sampling to increase the training frequency of images containing Unhealthy instances.
Apply targeted augmentation only to training images containing minority-class objects while retaining valid bounding boxes.
Initialize YOLOv8s with the Ultralytics detection framework.
Initialize Faster R-CNN with a ResNet-50 FPN backbone using the torchvision detection framework.
FOR each model m in {YOLOv8s, Faster R-CNN} DO
Train m for 150 epochs using its specified batch size, optimizer, learning rate, and scheduler.
Validate m after each epoch and monitor loss convergence and validation mAP.
Save the best checkpoint based on validation performance.
END FOR
FOR each best checkpoint m DO
Run inference on the independent test set under the controlled benchmark protocol.
Match predicted bounding boxes with ground-truth boxes using IoU thresholds.
Compute Precision, Recall, F1-score, mAP@50, mAP@50-95, and inference time.
END FOR
Compare YOLOv8s and Faster R-CNN based on detection accuracy, localization robustness, and computational efficiency.
Select M* as the model that provides the most appropriate accuracy-speed trade-off for UAV-based oil palm health monitoring.
END

3.2. Dataset

In this study, the dataset was obtained through the Roboflow platform and consists of a set of UAV images having a resolution of 1280x720 pixels and coming in RGB format, mainly showing the health condition of oil palm plants. The dataset that we've used consists of two main parts: Healthy and Unhealthy, which indicate plant physiological differences through leaf color, canopy pattern, and visible symptoms of stress due to different factors. Therefore, in this research, the data was divided into three main parts: training, validation, and testing. Different shares of the pictures and annotations were allocated to each portion: the training set contained 1,612 images (70% of the entire pool), the validation set 461 images (20%), and the test set was made up of 230 images (10%). Each photo was assigned to one of the two classes: healthy (0) indicating sound oil palm plants and unhealthy (1) signaling damaged ones. Within the training data, there were 104, 331 samples of healthy and 1, 563 samples of unhealthy, making a total of 105, 894 annotated samples. On average, there are about 65.7 object occurrences in each image of the training set. The validation and test datasets display similar figures with about 65 objects per image, as shown in table 2.

Table 2. Distribution of oil palm imagery datasets

Split	Number of images	Percentage	Instance Healthy (0)	Instance Unhealthy (1)	Total Instance	Average Instance/Image
Training	1,612	70%	104,331	1,563	105,894	65.7
Validasi	461	20%	29,563	421	29,984	64.9
Testing	230	10%	14,987	195	15,182	65.1

To ensure proper evaluation of model generalization, the images were split into training, validation, and testing subsets based on flight paths, not individual random images. Images captured from the same flight path were assigned exclusively to one subset to avoid overlap between subsets. This prevents the model from seeing visually similar images in both training and testing, ensuring that evaluation metrics reflect true generalization ability.

The split ratio remains the same: training set 70%, validation set 20%, and testing set 10%. Each subset contains images from distinct flight paths, as illustrated in table 3 below. This strategy ensures that adjacent images do not appear across multiple splits and eliminates potential data leakage.

Table 3. Breakdown of divisions by flight block

Split	Number of Flight Block	ID Flight Block	Criteria
Training	7	B01, B02, B03, B04, B05, B06, B07	70 %, area: Blocks do not overlap
Validation	2	B08, B09	20 %, area: Blocks do not overlap
Testing	2	B10, B11	20 %, area: Blocks do not overlap

3.3. Preprocessing and Labeling

The handling of data pretreatment and labeling was systematic and carefully done to ensure the best quality of data before the training of YOLOv8 and Faster R-CNN models [31]. Initially, the complete UAV image goes through multiple preprocessing steps, such as resizing to a fixed resolution, increasing visual quality by normalizing contrast, and using de-noising filters to eliminate lighting artifacts and wind disturbances of the palm canopy [32]. Labeling was done with the help of the Roboflow platform that provides a cloud-based annotation environment facilitating multi-annotator collaboration and centralized quality control [33]. In each image, a bounding box was drawn around the areas of leaves and bunches of fruits that indicate two classes of plant health: Healthy and Unhealthy, according to visual signs of plant stress [34]. To assure the consistency of the annotators, labeling guidelines were defined, including the smallest box size allowed, the exclusion of the background capture, and the grading criteria [35]. The dataset was then changed into two annotation formats; each one designed to the model's architectural needs: a standard coordinate YOLO format for YOLOv8 and a JSON-based COCO format capable of supporting multi-object structures and hierarchical information for Faster R-CNN [36]. By using the same preprocessing and labeling approaches, the resulting dataset is of high quality and ready for an impartial and thorough evaluation of the models' performance [37]. Figure 2 shows the results of the visualization of object annotations on aerial imagery (UAV) of oil palm fields. Each located oil palm was given a bounding box with two health categories: Healthy and Unhealthy.

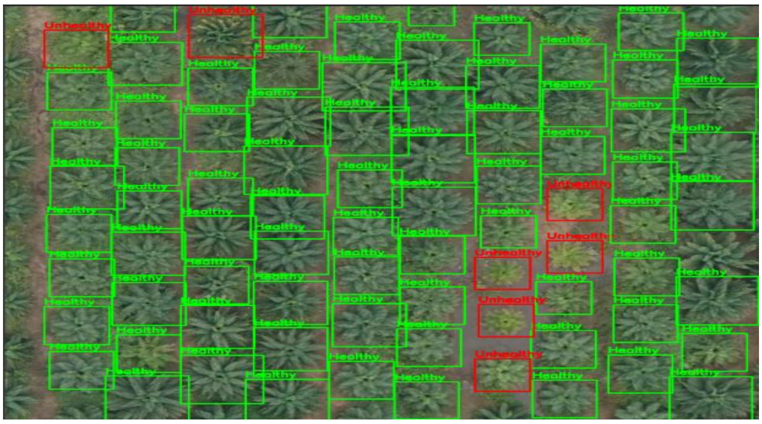

Figure 2. Visualization of UAV Image Annotation Results

3.4. Class Imbalance Handling

The dataset exhibited a substantial instance-level class imbalance between Healthy and Unhealthy oil palm categories. In the training subset, 104,331 Healthy instances and 1,563 Unhealthy instances were observed, corresponding to an imbalance ratio of approximately 66.75:1. Similar imbalance patterns were also found in the validation and testing

ISSN 2723-6471

subsets. Since such imbalance may bias the detector toward the dominant Healthy class, imbalance mitigation was incorporated during the training stage.

First, an image-level weighted sampling strategy was applied to increase the probability of selecting training images containing Unhealthy instances. This approach preserved the original bounding-box annotations while ensuring that minority-class samples appeared more frequently during mini-batch construction. Second, targeted data augmentation was applied to images containing Unhealthy objects, including random brightness and contrast adjustment, horizontal and vertical flipping, scale jittering, HSV variation, and random cropping while retaining valid bounding boxes. These augmentations were intended to increase the visual diversity of minority-class samples under different illumination, canopy texture, and viewing conditions.

Third, a class-sensitive learning strategy was adopted to reduce the dominance of the Healthy class during model optimization. For Faster R-CNN, class weights were incorporated into the classification loss based on inverse class frequency. For YOLOv8s, a focal-loss-based adjustment was used to increase the contribution of hard and minority-class examples during classification learning. The validation and testing sets were not oversampled or artificially balanced, so the reported performance reflects the natural class distribution encountered in field conditions.

3.5. YOLOv8s Training Setup

The YOLOv8s model was trained using the official Ultralytics implementation, which provides a modular and standardized interface for configuring YOLO-based object detection pipelines. The training process adopted the default Ultralytics hyperparameter configuration, including an initial learning rate of 0.01, a cosine learning rate scheduler, a batch size of 8, SGD optimization with momentum, and weight decay as a regularization mechanism. The model was trained for 150 epochs to ensure sufficient convergence of feature representations for detecting healthy and unhealthy oil palm trees from UAV imagery (see table 4). Although the training was conducted for 150 epochs, the loss curve indicated that YOLOv8s began to converge approximately around epoch 100. This distinction is important because the total training duration and the observed convergence point represent different aspects of the training process.

Table 4. YOLOv8s Training Setup

Parameter	**Configuration**
Framework	Ultralytics YOLOv8 (official implementation)
Training hyperparameters	Default Ultralytics configuration
Number of epochs	150
Batch size	8 (balanced for GPU memory and training stability)
Initial learning rate	0.01
Optimizer	SGD with momentum
Weight decay	Applied as regularization
Learning rate scheduler	Cosine scheduler
Notes	Trained for 150 epochs; convergence observed approximately around epoch 100

3.6. Faster R-CNN Training Setup

The Faster R-CNN model was implemented using the PyTorch-based torchvision detection framework. The architecture consisted of a two-stage detection pipeline combining a Region Proposal Network (RPN) with bounding box classification and regression heads. A ResNet-50 backbone integrated with a Feature Pyramid Network (FPN) was used and initialized with ImageNet-pretrained weights to support transfer learning on high-resolution UAV imagery. The model was trained for 150 epochs with a batch size of 4 due to the higher memory demand of the RPN and FPN components. The Adam optimizer was used with an initial learning rate of 0.01 and a weight decay of 1e-4, while a step-based learning rate scheduler was applied to stabilize gradient updates during fine-tuning. Compared with YOLOv8s, Faster R-CNN required a more computationally intensive training process because of its two-stage architecture, multi-resolution feature propagation, and non-maximum suppression procedures. All performance curves and loss analyses should be interpreted based on a total training duration of 150 epochs for both YOLOv8s and Faster R-CNN. References to epoch 98, epoch 99, or epoch 100 indicate observed convergence points or representative loss values during training, not the final number of training epochs. This clarification ensures consistency between the training setup descriptions, table 4 and table 5, and the interpretation of the model performance curves.

Table 5. Faster R-CNN Training Setup

Parameter	Configuration
Framework	Torchvision detection framework (PyTorch)
Architecture	Two-stage detector with RPN and bounding box classification/regression heads
Number of epochs	150
Batch size	4 (due to high memory usage for RPN & FPN)
Initial learning rate	0.01
Optimizer	Adam
Weight decay	1e - 4
Learning rate scheduler	Step-based LR scheduler
Notes	Trained for 150 epochs; computationally intensive due to RPN, FPN, ROI heads, and NMS

3.7. Evaluation Matrix

To evaluate the detection performance of YOLOv8s and Faster R-CNN in identifying healthy and unhealthy oil palm trees from UAV imagery, several standard object detection metrics were used, namely Precision, Recall, F1-score, Intersection over Union (IoU), mean Average Precision (mAP), and inference time [25]. These metrics were selected because they provide complementary information regarding classification correctness, detection sensitivity, localization accuracy, and computational efficiency. Precision measures the proportion of correctly detected positive samples among all samples predicted as positive [40]. It is calculated as follows:

Intersection over Union (IoU) is a fundamental metric used to evaluate the accuracy of object localization in detection tasks.

$$IoU = \frac{Area\ of\ overlap}{Area\ of\ union} \quad (1)$$

The Area of Overlap refers to the intersection between the predicted bounding box and the ground-truth box, while the Area of Union represents the total combined area covered by both boxes. IoU values range from 0 to 1, where higher values indicate better localization accuracy. In this study, IoU is used as the basis for computing evaluation thresholds such as mAP@0.5 and mAP@0.5:0.95, which assess detection performance under different levels of strictness whereas Average Precision (AP) was computed from the Precision–Recall curve for each class. The mean Average Precision (mAP) was then obtained by averaging AP values across all classes:

$$mAP = \frac{1}{N}\sum_{i=1}^{N} AP_1 \quad (2)$$

C denotes the number of classes and APc denotes the Average Precision of class ccc. In this study, mAP@0.5 refers to mAP calculated at an IoU threshold of 0.50, while mAP@0.5:0.95 refers to the average mAP calculated across IoU thresholds from 0.50 to 0.95 with a step size of 0.05. The latter provides a stricter evaluation of localization accuracy because it considers multiple IoU thresholds.

3.8. Controlled Inference Benchmark Protocol

To ensure a fair inference speed comparison, the YOLOv8 and Faster R-CNN models need to be evaluated using the same parameters, shown in table 6.

Table 6. Model Experiment Configuration

Components Benchmark	Information That Needs to Be Included
Test images	230 images
Input image size	640×640
Inference batch size	1
Hardware	RTX 3090, i9-12900K, 64 GB RAM
Software	Ubuntu 22.04, PyTorch 2.1, CUDA 12.0
Precision	FP32
Acceleration	No TensorRT/ONNX/quantization
Model mode	Evaluation mode
Warm-up iterations	10 iterations (GPU warm-up)
Timed repetitions	10 iterations (GPU warm-up)
Timing scope	[forward only / end-to-end]
NMS/confidence settings	10 iterations (GPU warm-up)
Warm-up iterations	10
Timed repetitions	100
Timing scope	Forward only
NMS/confidence settings	IoU=0.5, confidence=0.25

4. Results and Discussion

This part elaborates and explores deeply the results of performance measurement of the YOLOv8s and Faster R-CNN in detecting two classifications of oil palm plant health, Healthy and Unhealthy, through UAV imagery. Performed analysis includes the original as well as the augmented datasets to reflect field real-world and diverse operational situations. Using these two dataset types, the authors intended to set a standard of model performance and also understand the role of augmentation in making the model more invulnerable to visual changes of the oil palm canopy. This method of evaluation is very important for choosing the most effective and efficient models for large-scale smart agriculture applications in oil palm plantation areas.

4.1. Model test results with metrics precision, recall, mAP0.5, and mAP0.5:0.95

The final evaluation was done on a completely separate set of 230 UAV images that were taken from the training and validation datasets to show the comparative results of YOLOv8 and Faster R-CNN. The four main object detection metrics that are usually employed are precision, recall, mAP0.5, and mAP0.5:0.95. Precision measures a model's ability to reduce false positives, that is, to ensure that every object classified as a particular class is a real object of that class. This number is even more significant when it comes to oil palm plantations with very complex canopy structures that could confuse the detector. At the same time, recall measures the ability of a model to detect all objects present in the image, including very small and overlapping objects; therefore, this metric is necessary to understand the model's sensitivity to different variations in plant biology and morphology. The mAP 0.5 metric uses the Intersection over Union (IoU) threshold of 0.5 and shows how well object detection works when the overlap between the predicted boxes and the ground truth is high. It is essentially a first-level assessment of the object localization quality. Meanwhile, mAP 0.5:0.95 is a more demanding evaluation as it calculates the precision at various IoU thresholds between 0.5 and 0.95 and averages the results. Therefore, this metric reflects the model's capability of handling variations in distance and overlapping complexities in the region. By assessing these factors simultaneously, we will be able to conduct an indepth comparison between YOLOv8 and Faster R-CNN regarding their precision, object detection, and how well they adapt to different scenarios of oil palm plantations.

Figure 3 shows how the accuracy of two models has evolved over 150 epochs of training. For example, it is quite clear that the blue line representing YOLOv8s even during the first epoch went up very quickly and reached a precision of above 0.95 before going down again and finally settling almost at 1.00 which is quite a good indicator of the model being highly capable in not only reducing false positives but also keeping prediction reliability at a very high level. On the other hand, the red line for Faster R-CNN shows a decent initial progress but after that, the figure was stuck at a precision level of about 0.88, 0.90, hardly changing at all during the epochs, which in turn implies the model's struggle to cope with the complexities of palm canopy texture as well as varying light and different patterns of overlapping objects in UAV images. The ongoing disparities in performance prove that YOLOv8s has reached a higher level of accuracy in object classification, especially in agricultural or plantation environment with complicated foliage structures that can lead to false detections quite easily, thus making it a dependable model for UAV-based smart agriculture applications.

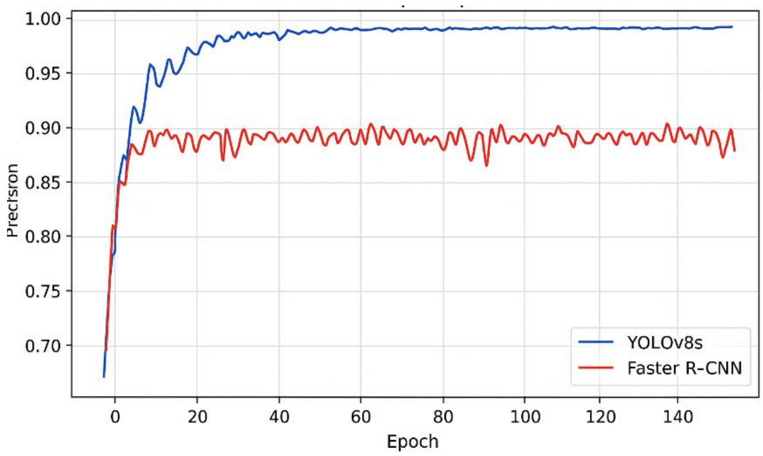

Figure 3. Precision metrics development curve

Figure 4 clearly shows that YOLOv8s (blue line) had a huge spike right at the beginning of the time period, meaning it achieved a recall close to 1.0 very fast, and it remained very stable at a high level during the whole training time. YOLOv8s is capable of recognizing almost every object in the UAV footage, including small, overlapping objects as well as those located in canopy areas with very complex texture variations. However, Faster R-CNN (red line) was stable only within the recall range of 0.70-0.75, and there were considerable decreases at the beginning of the training period, which imply its failure in detection consistency of objects in varied spatial conditions. The low recall of Faster R-CNN means that the model is missing more real objects as compared to YOLOv8, so it can be considered less suitable for plant health monitoring applications that require very sensitive visual changes and leaf morphology detection in aerial images.

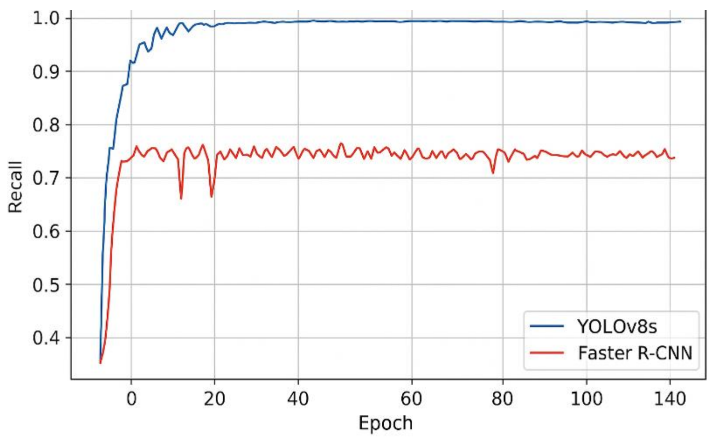

Figure 4. Recall metrics progression curve

The first phase (epoch 0-20) shown in figure 5 reveals a big improvement for both models; however, YOLOv8s (blue line) reaches a mAP@0.5 higher than 0.95 sooner and then stabilizes around 0.98-1.00, which shows that the model is able to predict the position of the object with a high degree of accuracy and with a lot of overlap with the ground truth. On the other hand, Faster R-CNN (red line) reached the level of 0.90-0.92 and showed more changes which means that the model struggling to keep a steady performance in detecting the objects in the UAV data which is characterized by complex variations of canopy, leaf textures and lighting conditions. The fact that the YOLOv8s curve is always above the Faster R-CNN curve at all the epochs indicates that YOLOv8s has better localization capabilities, is more resistant to changes in spatial variations of objects, and is more effective in detecting both healthy and stressed crop areas in oil palm plantation environments.

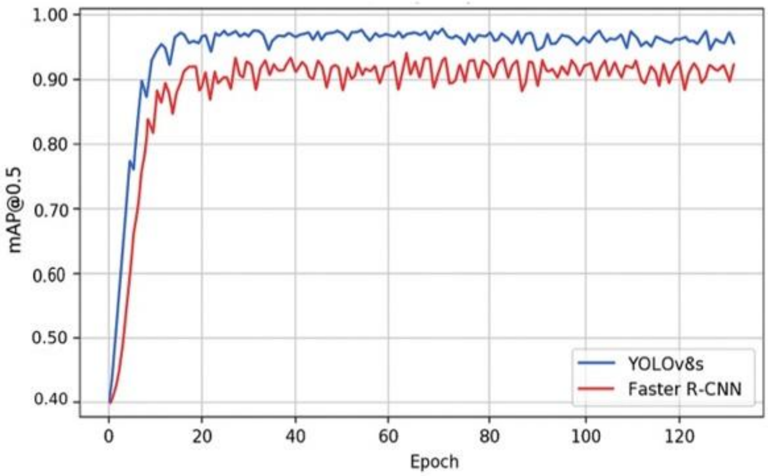

Figure 5. Metrics development curve mAP@0.5

Figure 6 illustrates the 0.5:0.95 mAP metric growth curve showing that localisation capability and the resilience of object identification between the two models differ substantially as the training of models progresses to 140 epochs. Initially, YOLOv8s (blue line) showed a rapid progress, quite fastly reached a mAP value of 0.5:0.95 more than 0.90, subsequently remained very stable in the range of 0.93, 0.95. This indicates that the model can maintain excellent detection accuracy at diverse IoU levels, even in cases of high object overlaps where precision is a must. However, on the opposite side, Faster R-CNN (red line) touched the levels of 0.80, 0.83 and besides that, it exhibited quite significant oscillations during the epochs, which is a hint that the model has some restrictions in accurately locating objects in real-life conditions of UAV imagery, like palm canopies that are crowded, irregular shadows, and different arrangements spatially of leaves, among other things. These lasting differences show that YOLOv8s not only have better reliability but also better generalization in coping with overlapping variations and object geometry in a plantation environment making them a better and more versatile model for UAV-based crop health assessment.

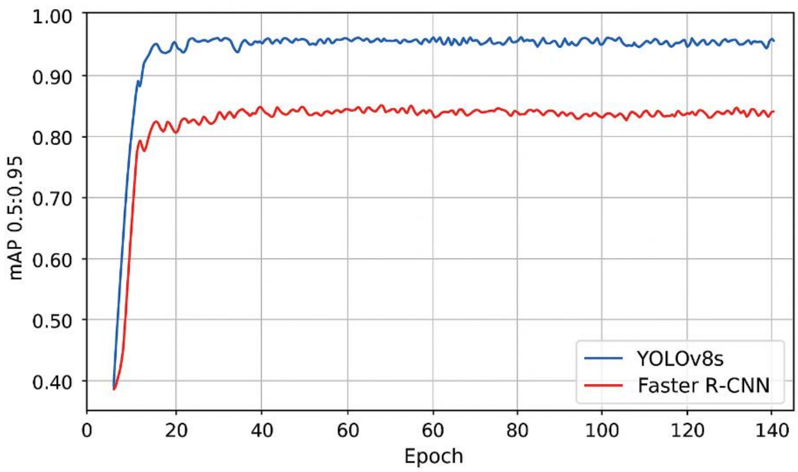

Figure 6. Growth curve metrics mAP 0.5:0.95

4.2. Model test results with loss function analysis

Loss function analysis was conducted to examine the convergence behavior and optimization stability of each model during training. However, because YOLOv8s and Faster R-CNN are based on different detection architectures and optimize different objective functions, their absolute loss values should not be interpreted as directly comparable indicators of accuracy. In this study, loss curves were therefore used only to assess model-specific learning dynamics, while cross-model performance comparison was based on common test-set metrics, namely precision, recall, mAP@50, mAP@50-95, and inference time.

For YOLOv8s in figure 7, the loss curve showed a rapid and stable decline during the early training epochs, indicating efficient convergence of the model within its one-stage detection framework. The decreasing box and classification losses suggest that YOLOv8s progressively improved its bounding-box regression and class prediction during training. Nevertheless, these loss values were interpreted only within the YOLOv8s training context and were not used as direct evidence of superiority over Faster R-CNN. For Faster R-CNN in figure 7, the loss curve showed a more gradual convergence pattern, which is consistent with its two-stage detection mechanism involving region proposal generation and subsequent object classification and bounding-box refinement. The reduction in Faster R-CNN loss indicates that the model successfully optimized its internal RPN and ROI-head components. However, the lower final classification loss observed in Faster R-CNN should not be interpreted as higher classification accuracy than YOLOv8s because the two models optimize different loss formulations.

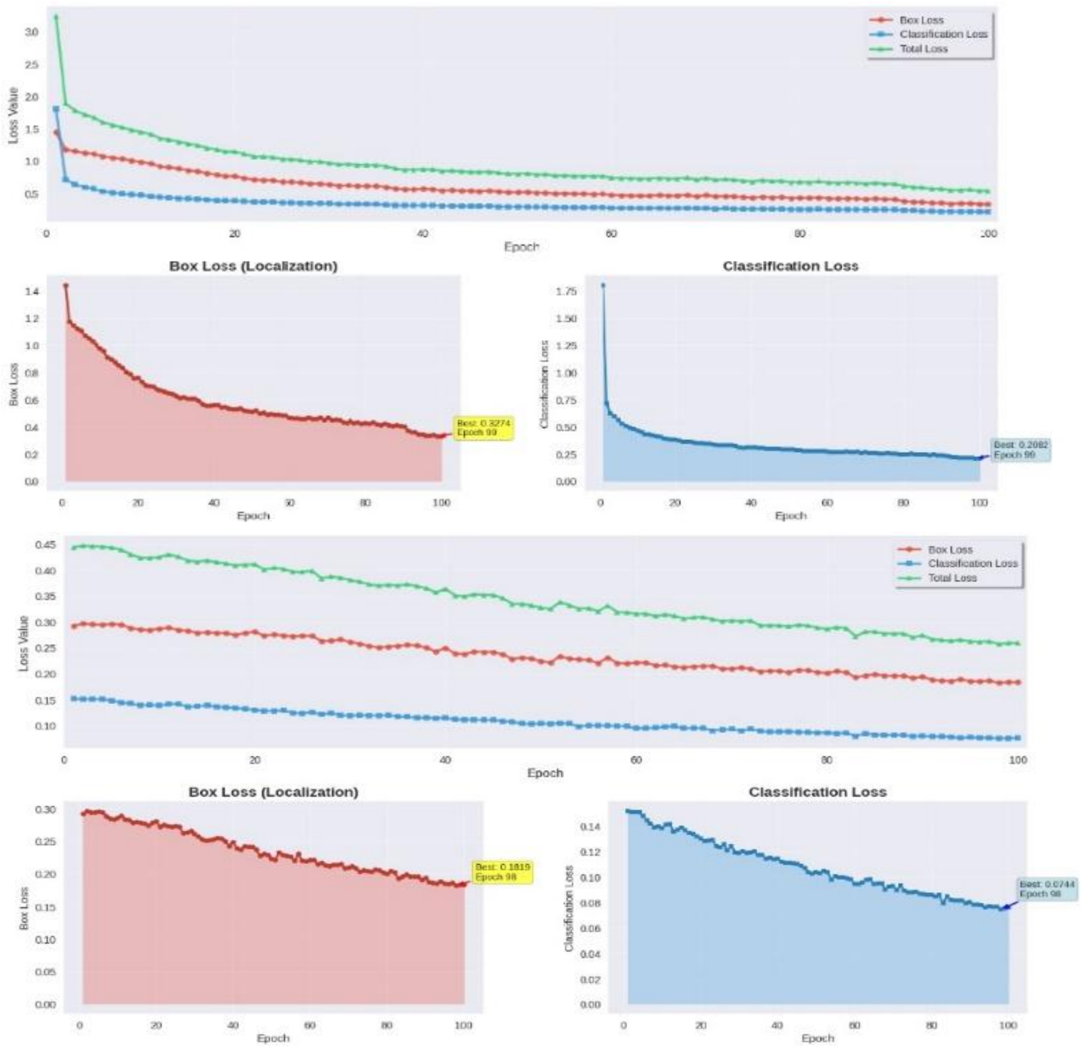

Figure 7. Summarizes the comparative performance metrics. Loss Function Analysis on YOLOv8 and Loss Function Analysis on Faster R-CNN

Therefore, the loss analysis supports the discussion of convergence stability and training behavior only (figure 8). The conclusion regarding comparative detection performance is drawn from the shared evaluation metrics on the same test set. Based on precision, recall, mAP@50, mAP@50-95, and inference speed, YOLOv8s demonstrated stronger overall suitability for real-time UAV-based oil palm health detection, while Faster R-CNN remains relevant for offline verification tasks that can tolerate higher computational cost.

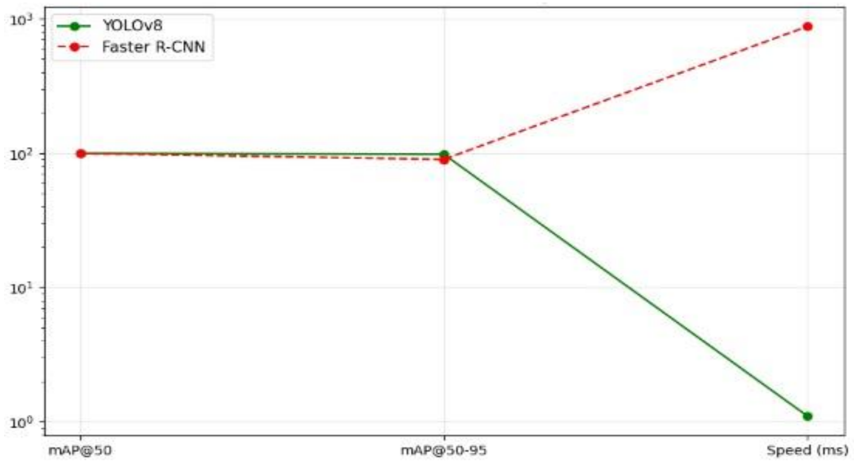

Figure 8. Chart Accuracy versus speed trade-off chart

4.3 Model test results with performance matrix

The data in table 7 shows that YOLOv8 excels in all metrics, especially for the Unhealthy class, with significant differences in precision, recall, F1-score, mAP@50, and mAP@50-95. This shows that YOLOv8 is more reliable in identifying plants that are under stress or damage than Faster R-CNN, especially in complex conditions such as overlapping objects, shadows, and canopy variations. The biggest advantage is seen in the mAP@50-95, which emphasizes that YOLOv8 is more effective in maintaining detection accuracy at various IoU thresholds, making it well-suited for real-time deployment in the field with UAV imagery.

Table 7. Performance Matrix

Metric	YOLOv8 Healthy	YOLOv8 Unhealthy	Faster R-CNN Healthy	Faster R-CNN Unhealthy	Delta YOLOv8-Unhealthy vs Faster
Precision	0.990	0.950	0.985	0.860	+0.09
Recall	0.995	0.890	0.992	0.780	+0.11
F1-Score	0.992	0.920	0.988	0.820	+0.10
mAP@50	0.995	0.960	0.993	0.870	+0.09
mAP@50-95	0.980	0.930	0.895	0.760	+0.17

Table 8 compares the health detection performance of oil palms using YOLOv8 and Faster R-CNN models on various environmental conditions that affect accuracy, such as the complexity of canopies, shadows, and overlapping objects. Data shows that YOLOv8 consistently has a higher mAP@50 and mAP@50-95 than Faster R-CNN in all conditions, in both easy (Low) and difficult (High) scenarios. The performance difference (Δ mAP) indicates the advantages of YOLOv8 especially at mAP@50-95, reflecting its better ability to handle distance variations, object overlaps, and complex canopy conditions. This trend confirms that YOLOv8 is more stable, reliable, and superior for real-time crop health monitoring applications using UAV imagery, while Faster R-CNN remains relevant for offline analysis despite its declining performance under difficult conditions.

ISSN 2723-6471

Table 8. Ablation Study

Factor	Subset	YOLOv8 mAP@50	YOLOv8 mAP@50-95	Faster R-CNN mAP@50	Faster R-CNN mAP@50-95	Δ mAP@50	Δ mAP@50-95
Canopy Complexity	Low	0.994	0.977	0.993	0.896	+0.001	+0.081
	High	0.992	0.970	0.990	0.880	+0.002	+0.090
Shadows	Low	0.994	0.977	0.993	0.896	+0.001	+0.081
	High	0.991	0.968	0.989	0.875	+0.002	+0.093
Overlapping Objects	Low	0.994	0.977	0.993	0.896	+0.001	+0.081
	High	0.990	0.965	0.987	0.870	+0.003	+0.095

5. Conclusion

Health assessment of oil palm plants from high-resolution UAV images. This study reveals that YOLOv8 is the fastest one among the models in terms of inference and convergence while it is also more computationally efficient than Faster R-CNN that is markedly the slowest and consumes the most of the CPU resources. Although Faster R-CNN achieves a slightly higher final accuracy, YOLOv8 is the most suitable for field situations where it is required to get quick and efficient detections. Limitations of this research are mainly lighting variabilities and field conditions which are not fully reflected in the utilized dataset. Such changes can affect the model's performance when it is exposed to more varied real-world situations. Besides, Faster R-CNN also faces challenges related to inference speed, which make it less suitable for scenarios where real-time response is critical. Development of a multi-class model that can identify various plant health conditions apart from 'healthy' and 'unhealthy' is going to be the most suitable step for the next paper. Also, employment of multispectral imagery might introduce a more detailed level of information on plant physiological stress that is not detectable by normal RGB imagery. Similarly, lightweight architectures that can be deployed on edge devices for drone-based automated field monitoring could be explored through continued research.

6. Declarations

6.1 Author Contributions

Conceptualization: K.Y.; Methodology: D.M.; Software: H.; Validation: K.Y. and D.M.; Formal Analysis: D.M. and H.; Investigation: K.Y.; Resources: D.M; Data Curation: H.; Writing Original Draft Preparation: K.Y., and D.M.; Writing Review and Editing: D.M., and H.; Visualization: K.Y.; All authors have read and agreed to the published version of the manuscript.

6.2 Data Availability Statement

The data presented in this study are available on request from the corresponding author.

6.3 Funding

The authors received financial support from Yayasan Pesat Nabire (Grant No. 201/BP-YP/I/2026) for the research, authorship, and/or publication of this article

6.4 Institutional Review Board Statement

Not applicable.

6.5 Informed Consent Statement

Not applicable.

6.6 Declaration of Competing Interest

The authors declare that they have no known competing financial interests or personal relationships that could have appeared to influence the work reported in this paper.

References

[1] R. Guebsi, S. Mami, and K. Chokmani, "Drones in precision agriculture: A comprehensive review of applications, technologies, and challenges," *Drones*, vol. 8, no. 11, pp. 1-30, 2024, doi: 10.3390/drones8110686.

[2] P. Ahmadi, S. Mansor, B. Farjad, and E. Ghaderpour, "Unmanned Aerial Vehicle (UAV)-based remote sensing for early-stage detection of Ganoderma," *Remote Sens.*, vol. 14, no. 5, pp. 1-15, 2022, doi: 10.3390/rs14051239.

[3] V. G. Dhanya, A. Subeesh, N. L. Kushwaha, D. K. Vishwakarma, T. N. Kumar, G. Ritika, and A. N. Singh, "Deep learning based computer vision approaches for smart agricultural applications," *Artificial Intelligence in Agriculture*, vol. 6, no 2022, pp. 211–229, 2022, doi: 10.1016/j.aiia.2022.09.007.

[4] Y.-A. Daraghmi, W. Naser, E. Y. Daraghmi, and H. Fouchal, "Drone-assisted plant stress detection using deep learning: A comparative study of YOLOv8, RetinaNet, and Faster R-CNN," *AgriEngineering*, vol. 7, no. 8, Art. no. 257, pp. 1-18, 2025, doi: 10.3390/agriengineering7080257.

[5] O. Doll and A. Loos, "Comparison of object detection algorithms for livestock monitoring of sheep in UAV images," in *Proc. Camera Traps, AI, and Ecology – 3rd Int. Workshop*, Jena, Germany, vol. 2023, no. September, pp. 7–8, 2023, doi: 10.24406/publica-2164.

[6] H. Zhu, C. Lin, G. Liu, D. Wang, S. Qin, A. Li, J.-L. Xu, and Y. He, "Intelligent agriculture: Deep learning in UAV-based remote sensing imagery for crop diseases and pests detection," *Frontiers in Plant Science*, vol. 15, no. October, Art. no. 1435016, pp. 1-24, 2024, doi: 10.3389/fpls.2024.1435016.

[7] J. Gao, K. Gujarati, M. Hegde, P. Arra, S. Gupta, and N. Buch, "Integration of UAV and remote sensing data for early diagnosis and severity mapping of diseases in maize crop through deep learning and reinforcement learning," *Remote Sensing*, vol. 17, no. 20, Art. no. 3427, pp. 1-32, 2025, doi: 10.3390/rs17203427.

[8] B. Alsadik, F. J. Ellsäßer, M. Awawdeh, A. Al-Rawabdeh, L. Almahasneh, S. Oude Elberink, D. Abuhamoor, and Y. Al Asmar, "Remote sensing technologies using UAVs for pest and disease monitoring: A review centered on date palm trees," *Remote Sensing*, vol. 16, no. 23, Art. no. 4371, pp. 1-20, 2024, doi: 10.3390/rs16234371.

[9] J. Agrawal and M. Y. Arafat, "Transforming Farming: A Review of AI-Powered UAV Technologies in Precision Agriculture," *Drones*, vol. 8, no. 11, pp. 1-25, 2024, doi: 10.3390/drones8110664.

[10] X. Yang, J. Chen, X. Lu, H. Liu, Y. Liu, X. Bai, L. Qian, and Z. Zhang, "Advances in UAV remote sensing for monitoring crop water and nutrient status: Modeling methods, influencing factors, and challenges," *Plants*, vol. 14, no. 16, Art. no. 2544, pp. 1-30, 2025, doi: 10.3390/plants14162544.

[11] L. Kouadio, M. El Jarroudi, Z. Belabess, S.-E. Laasli, M. Z. K. Roni, I. D. I. Amine, N. Mokhtari, F. Mokrini, J. Junk, and R. Lahlali, "A review on UAV-based applications for plant disease detection and monitoring," *Remote Sensing*, vol. 15, no. 17, Art. no. 4273, pp. 1-23, 2023, doi: 10.3390/rs15174273.

[12] T. B. Shahi, C.-Y. Xu, A. Neupane, and W. Guo, "Machine learning methods for precision agriculture with UAV imagery: A review," *Electronic Research Archive*, vol. 30, no. 12, pp. 4277–4317, 2022, doi: 10.3934/era.2022218.

[13] H. Chen, Y. Lan, B. K. Fritz, W. C. Hoffmann, and S. Liu, "Review of agricultural spraying technologies for plant protection using unmanned aerial vehicle (UAV)," *Int. J. Agric. Biol. Eng.*, vol. 14, no. 1, pp. 38–49, 2021, doi: 10.25165/j.ijabe.20211401.5714.

[14] B. R. Amogi, R. Ranjan, and L. R. Khot, "Mask R-CNN aided fruit surface temperature monitoring algorithm with edge compute enabled internet of things system for automated apple heat stress management," *Information Processing in Agriculture*, vol. 11, no. 4, pp. 603–611, 2024, doi: 10.1016/j.inpa.2023.12.001.

[15] A. Sharma, V. Kumar, and L. Longchamps, "Comparative performance of YOLOv8, YOLOv9, YOLOv10, YOLOv11 and Faster R-CNN models for detection of multiple weed species," *Smart Agricultural Technology*, vol. 9, no. December, pp. 1-14, 2024, doi: 10.1016/j.atech.2024.100648.

[16] R. Silva and P. Melo-Pinto, "t-SNE: A study on reducing the dimensionality of hyperspectral data for the regression problem of estimating oenological parameters," *Artificial Intelligence in Agriculture*, vol. 7, no. March, pp. 58–68, 2023, doi: 10.1016/j.aiia.2023.02.003.

[17] X. J. Tan, W. L. Cheor, K. S. Yeo, and W. Z. Leow, "Expert systems in oil palm precision agriculture: A decade systematic review," *Journal of King Saud University–Computer and Information Sciences*, vol. 34, no. 4, pp. 1569–1594, 2022, doi: 10.1016/j.jksuci.2022.02.006.

[18] S. N. A. M. Johari, S. Khairunniza-Bejo, A. R. M. Shariff, N. A. Husin, M. M. M. Masri, and N. Kamarudin, "Detection of bagworm infestation area in oil palm plantation based on UAV remote sensing using machine learning approach," *Agriculture*, vol. 13, no. 10, pp. 1-21, 2023, doi: 10.3390/agriculture13101886.

[19] A. Syetiawan, D. B. Susetyo, Y. Lumban-Gaol, Susilo, M. Ardha, Y. Susilo, and Wahono, "Deep learning-based palm tree detection in unmanned aerial vehicle imagery with Mask R-CNN," *TELKOMNIKA (Telecommunication Computing Electronics and Control)*, vol. 23, no. 1, pp. 156–165, 2025, doi: 10.12928/TELKOMNIKA.v23i1.26244.

[20] S. S. Lee, L. G. Lim, S. Palaiahnakote, J. X. Cheong, S. S. M. Lock, and M. N. Ayub, "Oil palm tree detection in UAV imagery using an enhanced RetinaNet," *Computers and Electronics in Agriculture*, vol. 227, no. December, pp. 1-13, 2024, doi: 10.1016/j.compag.2024.109530.

[21] K. Yarak, A. Witayangkurn, K. Kritiyutanont, C. Arunplod, and R. Shibasaki, "Oil palm tree detection and health classification on high-resolution imagery using deep learning," *Agriculture*, vol. 11, no. 2, pp. 1-16, 2021, doi: 10.3390/agriculture11020183.

[22] A. Haq, E. S. Cahyadi, M. S. Kasyfillah, R. Sarno, and A. T. Haryono, "Multi-class oil palm trees condition detection from UAV images using Faster R-CNN with EfficientNetV2," in *Proc. 2nd Int. Conf. Technology Innovation and Its Applications (ICTIIA)*, vol. 2024, no. December, pp. 1–6, 2024, doi: 10.1109/ICTIIA61827.2024.10761449.

[23] J. Kurihara, V.-C. Koo, C. W. Guey, Y. P. Lee, and H. Abidin, "Early detection of basal stem rot disease in oil palm tree using unmanned aerial vehicle-based hyperspectral imaging," *Remote Sensing*, vol. 14, no. 3, pp. 1-17, 2022, doi: 10.3390/rs14030799.

[24] N. H. Noordin, R. Samad, and A. H. A. Malek, "Real-time FFB ripeness detection using IoT-enabled YOLOv8n on Raspberry Pi 4 edge devices for precision agriculture," *Journal of Mechatronics, Electrical Power, and Vehicular Technology*, vol. 16, no. 2, pp. 305–317, 2025, doi: 10.55981/j.mev.2025.1220.

[25] A. Lahmdani, A. Elboushaki, and S. Saoud, "Targeted detection of plant disease infection levels using YOLOv8 and YOLOv9 for agricultural monitoring and public healthcare support," *Discover Artificial Intelligence*, vol. 6, no. February, Art. no. 258, pp. 1-15, 2026, doi: 10.1007/s44163-026-00841-z.

[26] G. Tariku, I. Ghiglieno, A. Simonetto, F. Gentilin, S. Armiraglio, G. Gilioli, and I. Serina, "Advanced image preprocessing and integrated modeling for UAV plant image classification," *Drones*, vol. 8, no. 11, Art. no. 645, pp. 1-18, 2024, doi: 10.3390/drones8110645.

[27] A. R. M. Amen, A. Mustafa, D. A. Kareem, H. M. Hameed, A. A. Mirza, M. Szydlowski, and B. K. M. Saleem, "Mapping of flood-prone areas utilizing GIS techniques and remote sensing: A case study of Duhok, Kurdistan Region of Iraq," *Remote Sensing*, vol. 15, no. 4, Art. no. 1102, pp. 1-20, 2023, doi: 10.3390/rs15041102.

[28] A. K. Kausik, A. B. Rashid, R. F. Baki, and M. M. J. Maktum, "Machine learning algorithms for manufacturing quality assurance: A systematic review of performance metrics and applications," *Array*, vol. 26, no. July, Art. no. 100393, pp. 1-30, 2025, doi: 10.1016/j.array.2025.100393.

[29] X. Du, Y. Sun, Y. Song, W. Chi, L. Dong, and X. Zhao, "Impact of input image resolution on deep learning performance for side-scan sonar classification: An accuracy–efficiency analysis," *Remote Sensing*, vol. 17, no. 14, pp. 1-24, 2025, doi: 10.3390/rs17142431.

[30] Y. Lyu, X. Han, P. Wang, J.-Y. Shin, and M.-W. Ju, "Unmanned aerial vehicle-based RGB imaging and lightweight deep learning for downy mildew detection in kimchi cabbage," *Remote Sensing*, vol. 17, no. 14, Art. no. 2388, pp. 1-23, 2025, doi: 10.3390/rs17142388.

[31] T. B. Shahi, C.-Y. Xu, A. Neupane, and W. Guo, "Recent advances in crop disease detection using UAV and deep learning techniques," *Remote Sensing*, vol. 15, no. 9, pp. 1-29, 2023, doi: 10.3390/rs15092450.

[32] L. Ezzeddini, J. Ktari, T. Frikha, N. Alsharabi, A. Alayba, A. J. Alzahrani, A. Jadi, A. Alkholidi, and H. Hamam, "Analysis of the performance of Faster R-CNN and YOLOv8 in detecting fishing vessels and fishes in real time," *PeerJ Computer Science*, vol. 10, no. May, Art. no. e2033, pp. 1-15, 2024, doi: 10.7717/peerj-cs.2033.

[33] R. Tsekhmystro, V. Lukin, and D. Krytskyi, "UAV image denoising and its impact on performance of object localization and classification in UAV images," *Computation*, vol. 13, no. 10, Art. no. 234, pp. 1-25, 2025, doi: 10.3390/computation13100234.

[34] Z. Salman, A. Muhammad, M. J. Piran, and D. Han, "Crop-saving with AI: Latest trends in deep learning techniques for plant pathology," *Frontiers in Plant Science*, vol. 14, no. August, Art. no. 1224709, pp. 1-19, 2023, doi: 10.3389/fpls.2023.1224709.

[35] O. W. Kent, T. W. Chun, T. L. Choo, and L. W. Kin, "Early symptom detection of basal stem rot disease in oil palm trees using a deep learning approach on UAV images," *Computers and Electronics in Agriculture*, vol. 213, no. October, Art. no. 108192, pp. 1-12, 2023, doi: 10.1016/j.compag.2023.108192.

[36] J. E. Murrugarra-Llerena, L. N. Kirsten, and C. R. Jung, "Can we trust bounding box annotations for object detection?," in *Proc. IEEE/CVF Conf. Computer Vision and Pattern Recognition (CVPR) Workshops*, vol. 2022, no. September, pp. 4813–4822, 2022, doi: 10.1109/CVPR52688.2022.00474.

[37] J. Dong, J. Lee, A. Fuentes, M. Xu, S. Yoon, M. H. Lee, and D. S. Park, "Data-centric annotation analysis for plant disease detection: Strategy, consistency, and performance," *Frontiers in Plant Science*, vol. 13, no. December, Art. no. 1037655, pp. 1-19, 2022, doi: 10.3389/fpls.2022.1037655.